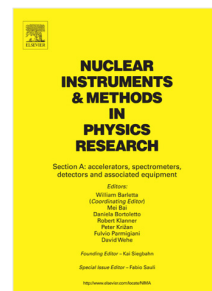


Accepted Manuscript

The hybrid MPGD-based photon detectors of COMPASS RICH-1

J. Agarwala, M. Alexeev, C.D.R. Azevedo, F. Bradamante, A. Bressan, M. Büchele, C. Chatterjee, M. Chiosso, A. Cicutin, P. Ciliberti, M.L. Crespo, S. Dalla Torre, S. Dasgupta, O. Denisov, M. Finger, M. Finger Jr., H. Fischer, M. Gregori, G. Hamar, F. Herrmann, S. Levorato, A. Martin, G. Menon, D. Panziera, G. Sbrizzai, S. Schopferer, M. Slunicka, M. Sulc, F. Tessarotto, J.F.C.A. Veloso, Y. Zhao



PII: S0168-9002(19)30111-1
DOI: <https://doi.org/10.1016/j.nima.2019.01.058>
Reference: NIMA 61832

To appear in: *Nuclear Inst. and Methods in Physics Research, A*

Received date: 21 November 2018
Revised date: 21 December 2018
Accepted date: 17 January 2019

Please cite this article as: J. Agarwala, M. Alexeev, C.D.R. Azevedo et al., The hybrid MPGD-based photon detectors of COMPASS RICH-1, *Nuclear Inst. and Methods in Physics Research, A* (2019), <https://doi.org/10.1016/j.nima.2019.01.058>

This is a PDF file of an unedited manuscript that has been accepted for publication. As a service to our customers we are providing this early version of the manuscript. The manuscript will undergo copyediting, typesetting, and review of the resulting proof before it is published in its final form. Please note that during the production process errors may be discovered which could affect the content, and all legal disclaimers that apply to the journal pertain.

The Hybrid MPGD-based photon detectors of COMPASS RICH-1

J. Agarwala^{a,j}, M. Alexeev^b, C.D.R. Azevedo^c, F. Bradamante^d, A. Bressan^d, M. Büchele^e, C. Chatterjee^d, M. Chiosso^b, A. Cicuttin^{a,j}, P. Ciliberti^d, M.L. Crespo^{a,j}, S. Dalla Torre^a, S. Dasgupta^a, O. Denisov^f, M. Finger^g, M. Finger Jr.^g, H. Fischer^e, M. Gregori^a, G. Hamar^a, F. Herrmann^e, S. Levorato^a, A. Martin^d, G. Menon^a, D. Panzieri^h, G. Sbrizzai^d, S. Schepfer^e, M. Slunicka^g, M. Sulcⁱ, F. Tassarotto^{a,*}, J.F.C.A. Veloso^c, Y. Zhao^a

^aINFN, Sezione di Trieste, Trieste, Italy

^bINFN, Sezione di Torino and University of Torino, Torino, Italy

^cIZN - Physics Department, University of Aveiro, Aveiro, Portugal

^dINFN, Sezione di Trieste and University of Trieste, Trieste, Italy

^eUniversität Freiburg, Physikalisches Institut, Freiburg, Germany

^fINFN, Sezione di Torino, Torino, Italy

^gCharles University, Prague, Czech Republic and JINR, Dubna, Russia

^hINFN, Sezione di Torino and University of East Piemonte, Alessandria, Italy

ⁱTechnical University of Liberec, Liberec, Czech Republic

^jAlso at Abdus Salam ICTP, 34151 Trieste, Italy

Abstract

Novel gaseous detectors of single photons for RICH applications have been developed and installed on COMPASS RICH-1 in 2016, covering a total area of 1.4 m². They have a hybrid architecture consisting of two staggered THGEM layers (one equipped with a CsI photoconverting layer) and a bulk Micromegas and operate stably and efficiently, providing a single photon angular resolution of ~ 1.8 mrad and about 10 detected photons per ring at saturation. The main aspects of their construction, commissioning, characterization and performance are presented.

Keywords: Photon detection, gaseous detectors, RICH, MPGD, THGEM, CsI photocathode

1. Introduction

The RICH-1 [1] detector of the COMPASS Experiment [2] at the CERN SPS is a large gaseous Ring Imaging Cherenkov counter providing hadron identification in the range of momenta between 3 and 60 GeV/c, over a large angular acceptance (± 200 mrad), at high rates (beam rate up to 100 MHz, trigger rate up to 100 kHz).

It consists of a 3 m long C₄F₁₀ radiator, a 21 m large focusing VUV mirror surface and Photon Detectors (PDs) covering a total active area of 5.5 m². Three photon detection technologies are used in RICH-1 (Fig. 1): Multi Wire Proportional Chambers (MWPCs) with CsI photocathodes, Multi Anode Photo-Multiplier Tubes (MAPMTs) and novel Micro Pattern Gaseous Detectors (MPGDs) based PDs.

The COMPASS RICH-1 was designed and built between 1996 and 2001 and is in operation since 2002. It was originally equipped with 16 PDs consisting in MWPCs hosting a CsI-coated photocathode, each having an active area of about 600×600 mm²; in 2006, to cope with the high particle flux of the central region, 4 such PDs were replaced by detectors consisting of arrays of MAPMTs coupled to individual fused silica lens telescopes.

In parallel, an extensive R&D program [3], aimed to develop MPGD-based large area PDs, established a novel hybrid tech-

nology combining MicroMegas (MM) and Thick Gas Electron Multipliers (THGEMs), providing good stability in harsh operating conditions.

In 2016 The COMPASS RICH-1 was upgraded by replacing 4 MWPCs-based PDs with detectors resulting from the newly developed MM+THGEM hybrid technology [4]. MPGD-based detectors of single photons are used for the first time in a running experiment.

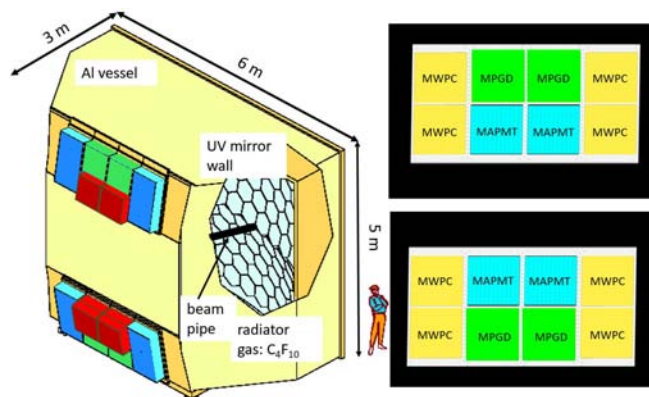


Figure 1: Artistic view of the COMPASS RICH-1 (left) and scheme of the PD arrangement (not in scale) (right).

*corresponding author, email: fulvio.tassarotto@ts.infn.it

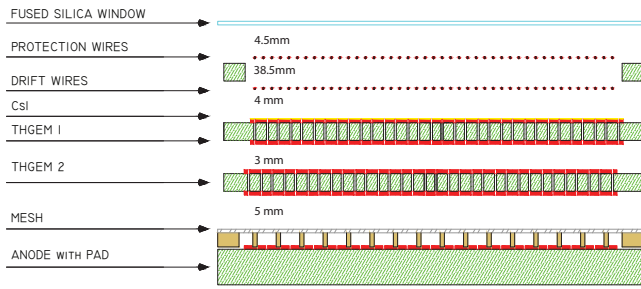
33 **2. The novel Hybrid MPGD-based Photon Detectors**

Figure 2: Sketch of the hybrid single photon detector: two THGEM layers are coupled to a MM. Drift and protection wire planes are shown. Image is not to scale.

34 The novel Hybrid MPGD-based PD architecture, sketched in
 35 Fig.2, consists in a combination of two layers of THGEM followed by a MM; the top of the first THGEM is coated with a
 36 CsI film and acts as a reflective photocathode. In this configuration the feedback from photons generated in the multiplication
 37 processes is suppressed by the presence of the THGEM layers and the large majority of the ions from the MM multiplication
 38 are collected at the MM mesh. The signal development time is about 100 ns.

43 Each of the four new COMPASS RICH-1 PDs has 600
 44 600 mm² and is formed by two identical modules (of 600
 45 300 mm²) arranged side by side.

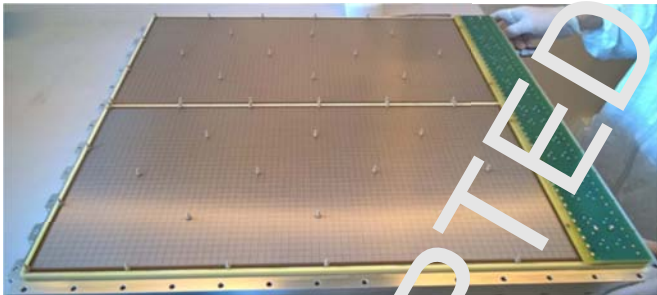


Figure 3: Two Micromegas mounted side by side in a PD. The pillars that preserve the distance between the micromesh and the THGEM above it are also visible.

46 The MMs (Fig.3) were produced at CERN using the bulk
 47 technology [5] on a custom, pad segmented anode; they have a
 48 128 μm gap and a square array of 200 μm diameter pillars with
 49 2 mm pitch.

50 The THGEMs (Fig.4) are made from standard PCB material
 51 and their geometrical parameters are: thickness = 470 μm (400
 52 μm dielectric, 2 \times 5 μm copper), hole diameter = 400 μm ,
 53 pitch = 800 μm ; the holes are rimless. The THGEM top and
 54 bottom electrodes are segmented in 12 parallel sectors, separated by 0.7 mm clearance, each biased via an individual (1 G Ω)
 55 resistor. The two THGEMs are staggered, providing maximal
 56 misalignment between the two set of holes: this configuration
 57 increases the PD electrical stability.

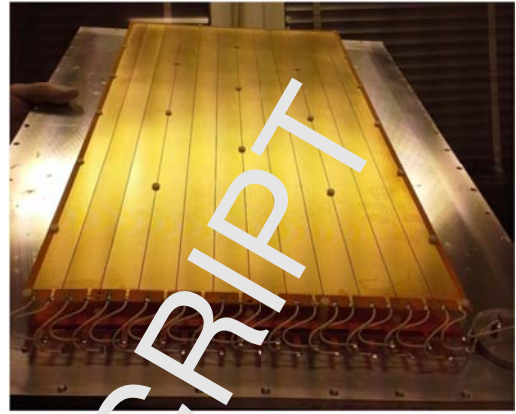


Figure 4: A Au coated THGEM ready for insertion in the CsI evaporation plant.

59 A specific protocol for production and validation of the
 60 THGEMs has been applied, consisting in: preselection of
 61 raw PCB material for homogeneous thickness, polishing after
 62 drilling with fine pumice powder, cleaning with high pressure
 63 water and ultrasonic bath with a basic (pH11) solution, detailed
 64 optical inspection, test of electrical strength, measurement of
 65 gain uniformity and long test of discharge rates under illumination
 66 by X-rays. The selected THGEMs were then coated with
 67 Ni (5 nm) and Au (0.2 μm) (Fig.4); half of them were subject to
 68 a further coating with a 300 nm CsI layer to become reflective
 69 photocathodes. The quantum efficiency (QE) of the CsI photocathodes
 70 is measured inside the evaporation plant after the coating process:
 71 the uniformity level is $\pm 3\%$ r.m.s. within a photocathode and
 72 $\pm 10\%$ between different photocathodes. To preserve the QE all
 73 operations of transport and installation are performed under controlled
 74 atmosphere, in dedicated glove-boxes.

76 The hybrid PD anode is segmented in 7.5 \times 7.5 mm² pads
 77 with 0.5 mm interpad clearance and each pad is biased at positive
 78 voltage (~ 620 V) via an individual (470 M Ω) resistor; the MM
 79 micromesh, being the only non-segmented electrode, is kept at ground
 80 potential. This configuration prevents occasional discharges from
 81 propagating to neighboring pads, limits the voltage drop suffered
 82 by the pads surrounding a tripping one to about 2 V, (corresponding
 83 to a gain drop $\sim 4\%$) and allows restoring the nominal voltage in
 84 few seconds. It also allows normal operation of the detector even
 85 when an anodic pad is shorted to ground potential (a few cases
 86 appeared during the runs 2016 and 2017, resulting in a total of less
 87 than 0.1% dead MM area). The signal is transmitted from the anode
 88 pad via capacitive coupling to a readout pad facing it, buried inside
 89 the anode PCB (at 70 μm distance from the anode pad) and connected
 90 to the front-end board connector. The resistive-capacitive pad
 91 scheme dumps the effects of discharges and protects the front-end
 92 electronics.

94 The novel hybrid PDs are operated with an Ar/CH₄ = 50/50
 95 gas mixture. The ion back-flow to the THGEM photocathode, in
 96 the standard operating conditions has been measured to be
 97 3% (Fig.5) by recording the currents on each electrode of the
 98 hybrid PD using a set of custom, fully floating, picoammeters.

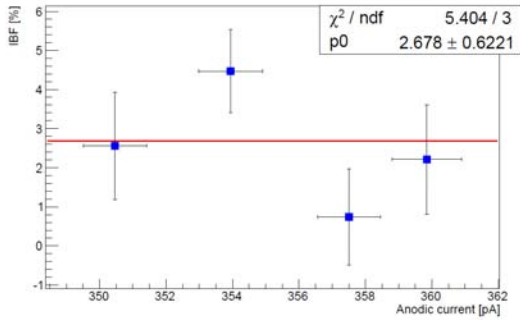


Figure 5: Dedicated measurement of ion back-flow fraction to the THGEM photocathode at four different values of the UV light intensities.

3. The commissioning of the MPGD-based PDs

The new PDs have been installed on COMPASS RICH-1 during Spring 2016, commissioned during the 2016 run, and operated stably and efficiently during the 2017 run too. The high voltage is provided by commercial power suppliers (CAEN A1561HDN and A7030DP HV modules, hosted in two SY4527 mainframes); each chamber is divided into 4 independent sectors and has 9 different electrode types, each one having specific requirements.

The HV control system (custom made, using C++ and wxWidgets) monitors and records at 1 Hz frequency the voltage and current values of all the 136 channels, counts the discharges (events with ≥ 20 nA current increase) and reconfigures automatically the specific voltage bias in case the discharge rate exceeds the allowed limit. It also measures the variation of environmental parameters (pressure and temperature) and provides automatic voltage adjustment to compensate for it, in order to preserve the stability of the PD gain. Discharges typically affect single sectors, reach a maximum current of about 100 nA and need ~ 10 s to restore the operating conditions. Their rate is about 1/h per chamber. Discharges in the two THGEM layers are fully correlated, and those observed in the MM are mostly related with the THGEM ones. No high voltage power supply protection trips ($I \geq 100$ nA for more than 10 s) were observed during data taking.

The front-end electronics [6], is based on the APV25-S1 chip, and provides three amplitude samples per trigger for each channel. Digitizer boards hosting 10 bit flash ADCs and FPGAs performing on-line zero suppression with common-mode correction send the detector data to the COMPASS DAQ for data storage and monitoring. A cooling system using under-pressure water flow assures efficient removal of the heat produced by the readout. The average noise level is ~ 800 equivalent e^- r.m.s, highly stable during the running periods. A clustering algorithm is applied in the analysis to provide coordinates and amplitudes of "photon candidate" clusters; the majority ($\geq 90\%$) of clusters however receive contribution from a single pad only.

The average effective gain of the 16 sectors was tuned to be the same (at 1% level) and remained stable at a level of 5% over several months of continuous operation thanks to the automatic

voltage adjustment to compensate for pressure and temperature changes. The ring images provided by the novel detectors are clean and almost background-free: typical examples are presented in Fig.6, where a ring fully contained in one of the new PDs (left) is shown together with a "shared" ring (right), namely a ring with photons detected mainly by the new PD and partly by the MAPMTs. In both cases the reconstruction and identification efficiency is satisfactory.

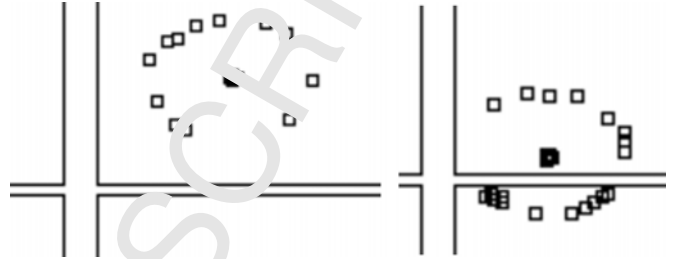


Figure 6: Examples of fully contained and shared rings

4. Preliminary performance results

A preliminary characterization of the hybrid THGEM-MM PD response has been performed from the analysis of data collected during two days of dedicated RICH calibration runs in September 2017; during this period the radiator gas consisted in a mixture of $C_4F_{10}/N_2 \sim 75/25$.

Photon candidate clusters contributing to the rings of identified particles are selected to obtain pure samples of Cherenkov photoelectron signals: an example of their amplitude distribution is presented in Fig.7 where the expected exponential behavior is observed over more than two orders of magnitude. The extracted value for the effective gain is ~ 14000 . The respective contributing factors from the three layers (first THGEM, second THGEM and MM) of electron multipliers to the effective gain are estimated to be $\sim 13, 9$ and 120 .

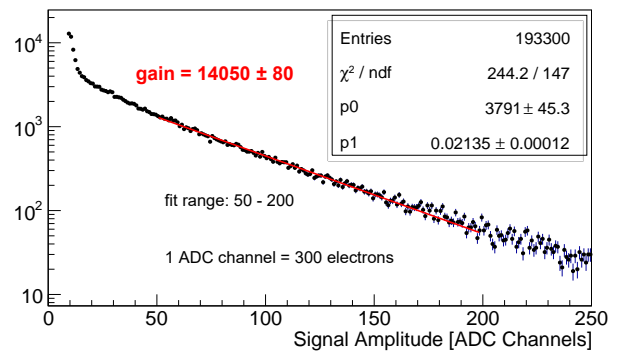


Figure 7: A typical signal amplitude distribution

The single photoelectron detection efficiency, estimated from the measured effective gain and the threshold applied to the signals, is $\geq 80\%$; the level of background hits in the ring coronas, originated by the electronic noise, is expected to be $\leq 20\%$: the observed deviation of the hit amplitude distribution from a pure exponential at very small amplitudes confirms this expectation.

169 Selecting identified pion rings, the detector angular resolution
 170 for single Cherenkov photoelectrons has been measured to
 171 be ~ 1.85 mrad, as can be seen in Fig. 8, where the difference
 172 between the Cherenkov angle calculated from the reconstructed
 173 momentum of the particle track and the measured Cherenkov angle
 174 for each photon candidate cluster is shown: this value fully
 175 matches the expectation. The use of a preliminary alignment
 176 results in an offset of 0.44 mrad.

177 The average number of detected photons per ring depends
 178 quadratically on the Cherenkov angle, according to the Frank-
 179 Tamm equation: the observed number of detected clusters
 180 shows the expected behavior, as can be seen in Fig. 9, where
 181 the points marked by triangles represent the measured quantities
 182 and the open circles include the correction for the effect of
 183 the non negligible probability of a statistical outcome of zero
 184 photons when the average is small. To increase the statistical
 185 accuracy of the estimate, the shared rings are used too, provided
 186 at least half of the ring corona is contained in the active area of
 187 the novel hybrid PD. The limited kinematic range of the pion
 188 data sample (momentum = 4.5 ± 1.4 GeV/c) and the effective re-
 189 fractive index of the radiator (~ 1.00127) provide a maximum
 190 observed Cherenkov angle of ~ 50 mrad. The reconstructed
 191 rings with large, unphysical angles are due to background hits
 192 and have a low number of photons per ring.

193 A fit of the corrected distribution with a quadratic (Frank-
 194 Tamm) + linear (random background proportional to the corona
 195 area) function is then performed in the range of Cherenkov angles
 196 where high statistical accuracy and small correction effects
 197 are present: since the quality of the fit is good and the level of
 198 background obtained from the fit agrees with the expectation,
 199 a preliminary estimate for the number of detected photons for
 200 tracks at saturation ($\beta=1$) can be reliably extracted. The curve
 201 shown in Fig. 9 provides a value of ~ 13 hits at a Cherenkov
 202 angle value of 55.2 mrad, which is the traditional reference
 203 Cherenkov angle value at saturation for CsI photomultiplier and
 204 a C_4F_{10} radiator at s.t.p.; the number of detected photons from
 205 the fit is ~ 10.5 and the background contribution is ~ 2.5 .

206 A complete characterization of the new detector is still on-
 207 going, but from the preliminary results a clear indication of a
 208 very stable and reasonably high effective gain, low noise level,
 209 good angular resolution and large photoelectron detection effi-
 210 ciency is obtained.

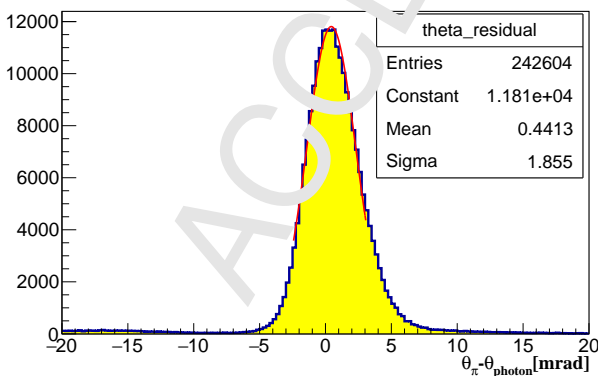


Figure 8: Detector angular resolution for single Cherenkov photons

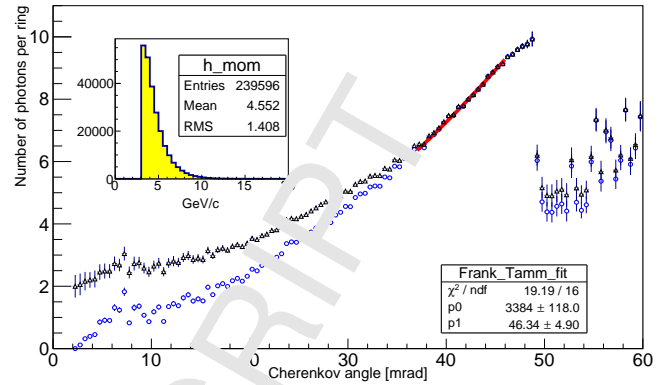


Figure 9: The average number of detected photons per ring as function of Cherenkov angle in a hybrid PD for identified pions. Triangular markers: measured values, open circles: corrected values. Top left box: distribution of the momenta of the identified pions

5. Conclusion

New large area gaseous detectors of single photons, based on a hybrid combination of THGEMs and Micromegas, have been developed and installed on COMPASS RICH-1 in 2016. They operate stably and efficiently with an effective gain of $\sim 1,000$, a noise level of ~ 800 equivalent e^- r.m.s., providing a single photon angular resolution of ~ 1.85 mrad and about 10 detected photons per ring at saturation.

They represent a remarkable technological achievement, since gaseous PDs are the most effective approach to instrument large surfaces with detectors of single photons at affordable costs, and they have a very low magnetic sensitivity.

MPGD-based photon detectors are a promising option for future RICH applications too.

Acknowledgements

The authors are grateful to the colleagues of the COMPASS Collaboration for continuous support and encouragement.

This work is partially supported by the H2020 project AIDA-2020, GA no. 654168.

References

References

- [1] E.Albrecht, *et al.*, Status and characterisation of COMPASS RICH-1, Nucl. Instrum. Meth. A **553** (2005) 215; P.Abbon *et al.*, Read-out electronics for fast photon detection with COMPASS RICH-1, Nucl. Instrum. Meth. A **587** (2008) 371; P.Abbon *et al.*, Design and construction of the fast photon detection system for COMPASS RICH-1, Nucl. Instrum. Meth. A **616** (2010) 21; P.Abbon *et al.*, Particle identification with COMPASS RICH-1, Nucl. Instr. and Meth. A **631** (2011) 26; F.Tessarotto *et al.*, Long term experience and performance of COMPASS RICH-1, JINST **9** (2014) C09011.
- [2] P. Abbon *et al.*, The COMPASS Experiment at CERN, Nucl. Instr. and Meth. A **577** (2007) 455; P. Abbon *et al.*, The COMPASS setup for physics with hadron beams, Nucl. Instr. and Meth. A **779** (2015) 69.

- 243 [3] M.Alexeev *et al.*, *The quest for a third generation of gaseous photon detectors*
244 *for Cherenkov imaging counters*, Nucl. Instr. and Meth. A **610** (2009)
245 174; M.Alexeev *et al.*, *THGEM based photon detector for Cherenkov*
246 *imaging applications*, Nucl. Instr. and Meth. A **617** (2010) 396; M.Alexeev
247 *et al.*, *Progress towards a THGEM-based detector of single photons*, Nucl.
248 *Instr. and Meth. A* **639** (2011) 130; M.Alexeev *et al.*, *Development of*
249 *THGEM-based Photon Detectors for COMPASS RICH-1*, Physics Procedia
250 37 (2012) **781**; M.Alexeev *et al.*, *MPGD-based counters of single photons*
251 *developed for COMPASS RICH-1*, JINST **9** (2014) C09017; M.Alexeev
252 *et al.*, *Long term experience with CsI photocathodes in gas photon detec-*
253 *tors*, JINST **9** (2014) P01006; M.Alexeev *et al.*, *The gain in Thick GEM*
254 *multipliers and its time-evolution*, JINST **10** (2014) P03026.
- 255 [4] M.Alexeev *et al.*, *The MPGD-based photon detectors for the upgrade of*
256 *COMPASS RICH-1*, Nucl. Instr. and Meth. A **876** (2017) 96.
- 257 [5] I.Giomataris *et al.*, *Micromegas in a bulk*, Nucl. Instrum. Meth. A **560**
258 (2006) 405.
- 259 [6] P.Abbon *et al.*, *Fast readout of the COMPASS RICH CsI-MWPC photon*
260 *chambers*, Nucl. Instr. and Meth. A **567** (2006), p. 104.